CONF-840604--10

ION BOMBARDMENT DAMAGE IN A MODIFIED Fe-9Cr-1Mo STEEL*

CONF-840604--10

DE84 014288

K. Farrell and E. H. Lee
Metals and Ceramics Division
Oak Ridge National Laboratory
Post Office Box X
Oak Ridge, Tennessee 37831 (USA)

ABSTRACT: A normalized-and-tempered Fe-9Cr-1Mo steel, modified with small quantities of niobium and vanadium, was bombarded with 4 MeV iron ions to a nominal displacement level of 100 dpa at temperatures of 400, 450, 500, 550, and 600°C. The major microstructural damage feature created in the lath-like α-ferrite grains was dislocation tangles which coarsened with increasing bombardment temperature. Sparse cavities were heterogeneously distributed at 500 and 550°C. Incorporation of helium and deuterium simultaneously in the bombardments at rates of 10 and 45 appm/dpa, respectively, introduced very high concentrations of small cavities at all temperatures, many of them on grain boundaries. These cavities were shown to be promoted by helium. A small fraction of the matrix cavities exhibited bias-driven growth at 500 and 550°C, with swelling <0.4%. This is a very narrow temperature range for bias-driven swelling. It is about 125°C higher than the peak swelling temperature found in neutron irradiations, which is compatible with the higher damage rate used in the ion bombardments. High concentrations of subgrain boundaries and dislocations resulting from the heat treatment, and unbalanced cavity and dislocation sink strengths in the damage structures contribute to the swelling resistance. Such resistance may not be permanent. High densities of bubbles on grain boundaries indicate a need for helium embrittlement tests.

KEY WORDS: Ferritic steel, heavy ion bombardments, swelling, microstructural damage, helium effects

---

*Research sponsored by the Division of Materials Sciences, U.S. Department of Energy under contract DE-AC05-840R21400 with Martin Marietta Energy Systems, Inc.

INTRODUCTION: Elevated temperature irradiation damage in ferritic steels has not been explored as extensively as that in austenitic steels. Nevertheless, the general trend of observations indicates that the ferritic alloys seem to have better resistance to cavitational swelling [1] and to helium embrittlement [2] than do austenitic alloys. One class of ferritic steels undergoing development and investigation for potential applications in high temperature power generators is the Fe-9Cr-1Mo system, modified by additions of niobium and vanadium and used in the normalized-and-tempered condition [3]. We have examined the response of one of these steels to heavy ion bombardment under conditions chosen to simulate fusion reactor-type irradiations involving high helium and hydrogen generation rates.

EXPERIMENTAL CONDITIONS: The steel was made by Combustion Engineering, Chattanooga (heat number 91887). Its chemical composition in wt % is Fe — 0.095C — 9.0 Cr — 0.95 Mo — 0.08 Ni - 0.1 Si - 0.39 Mn — 0.21 V — 0.18 Nb. Disks of 3 mm diameter were punched from 0.5 mm thick cold-rolled sheet. They were encapsulated in silica tubes in low-pressure argon, and were heated for 1h at 1038°C and air cooled, followed by reheating to 760°C for 1h and air cooling. These heat-treated disks were prepared for ion bombardment by mechanical polishing and a final electropolish. Bombardments were made in the ORNL dual ion facility [4] to a nominal displacement dose of 100 dpa with 4 MeV iron ions and concurrently with helium ions at a rate of 10 appm/dpa and with deuterium ions at a rate of 45 appm/dpa. To distinguish the effects of the gases, some specimens were bombarded with iron ions only. The nominal bombardment temperatures were 400, 450, 500, 550, and 600°C. Damage was examined by TEM at the peak damage depth of 0.9 μm.

RESULTS: The microstructure (Fig. 1) of the as-heat-treated specimens was typical of the normalized-and-highly tempered condition, consisting of many lath-shaped α-ferrite grains. The mean width of the laths was about 0.5 μm, with considerable variation around this mean. The laths were subdivided irregularly across their widths by sub-boundary-type dislocation networks, many of them discontinuous; their mean spacing along the lengths of the laths was about 0.5 μm. There were also numerous dislocations randomly intersecting one another at a density of 2–3 × $10^{14}/m^2$. The sites of large, equiaxed, prior austenite grain boundaries were decorated with lens-shaped second-phase particles. Electron diffraction patterns from these particles were consistent with those for the $M_{23}C_6$ phase. Such particles were also present on some of the lath boundaries and randomly within the laths. Aging treatments of 4.5 h at temperatures of 400 to 600°C to reproduce the heating conditions during bombardment caused no changes in the microstructure.

Bombardments with iron ions alone caused the formation of tightly-knitted dislocation tangles at 400 and 450°C. Looser dislocation tangles occurred at 500°C and less at 550°C. At 600°C, there was no obvious change in dislocation density from the as-heat-treated condition. Cavities were found only in the 500 and 550°C specimens. They were larger and fewer at 550°C than at 500°C. The spatial distribution of these cavities was highly heterogeneous. None were seen on grain boundaries. Most laths in a field of view contained no cavities, some regions held just one or two cavities, and some of the larger laths housed loose clusters of cavities in their central regions. The largest cluster observed in the 500°C specimen contained 3.5 × 10^{20} cavities/m^3, with a maximum diameter of 51 nm. Figure 2a shows some of these cavities but does not adequately depict

the nonuniform distribution. Table 1 lists some rough measurements of the microstructural damage features, together with the specific bombardment conditions pertaining at the peak damage depths. Because of the heterogeneous dispersion of the cavities and the low numbers sampled, these measurements are subject to considerable uncertainties. They are intended for comparative purposes, and should not be regarded as absolute values. A similar caution applies to the other data in Table 1.

Triple beam bombardments with iron, helium, and deuterium ions caused dislocation tangles and high concentrations of small cavities (Figs. 2b, c, and Table 1) at all five bombardment temperatures. These cavities were located within laths, on lath boundaries and on particle-matrix interfaces. The cavities were very small and difficult to resolve in the 400 and 450°C specimens where they embraced the working resolution limit of 1.5–2.0 nm. Consequently, many submicroscopic cavities may exist, too. Although the matrix cavities appeared to be uniformly distributed throughout the laths, many of the cavities at 550 and 600°C lay in lines and walls suggestive of sometime asociation with dislocation lines and networks. In general, the cavities decreased in concentration and increased in size with increasing bombardment temperatures. However, perturbations occurred in the 500 and 550°C specimens where a small fraction of the cavities ($\lesssim$10%) displayed exaggerated growth with respect to their companions. This biomodal growth is distinguished in Table 1 by diagonal lines separating the cavity measurements for the small and large size classes. The microstructures were essentially similar to that shown in Fig. 2b. The spatial arrangement of the larger cavities in the bimodal size distributions was nonuniform. While some were found in all laths, they occurred most frequently in the wider laths.

One dual beam bombardment with iron and helium ions was made at 500°C to see if withholding the deuterium beam would affect the outcome. The resulting damage microstructure (Fig. 2b) was qualitatively the same as that produced by the triple beam bombardment. The quantitative comparison (Table 1), which seems to show that more cavities were created in the dual beam bombardment than in the corresponding triple beam bombardment, is marred by probable sampling errors and by the fact that the displacement level in the former was more than twice that in the latter. This uncertainty does not affect the more important conclusion, i.e., enhanced cavity nucleation and bimodal cavity growth occurred in both the dual beam and triple beam irradiations. This indicates that helium strongly promotes the formation of cavities, and co-generation of hydrogen (deuterium) is not a necessary condition.

The matrix regions immediately adjacent to grain boundaries contained noticeably fewer cavities than regions deeper in the grains. The limits of these partially denuded regions were not well-defined but the widths increased with increasing bombardment temperature. Rough values were about 30 nm at 500°C, and about 70 nm at 600°C. The larger cavities in the laths tended to lie at farther distances from the grain boundaries than did the smaller cavities. Prior austenite and lath boundaries were liberally covered with cavities (Fig. 2c), generally smaller than those within the laths.

DISCUSSION: Despite the experimental uncertainties in these data, the measured differences in microstructural details between those bombardments made with iron ions alone and those made with simultaneous beams of iron and gases are so large as to leave no doubt that the gases have substantial influence on the development of the damage structure. We see that the major microstructural damage feature

in this ferritic steel after self-ion bombardments without gas is dislocation tangles. These tangles coarsen with increasing temperature and are not discernible for the 600°C bombardment, thus implying complete recombination of radiation-produced point defects at 600°C. Sparse cavities are formed only at 500 and 550°C. When helium and deuterium are incorporated in the bombardments at the high gas/dpa rates predicted for fusion reactor conditions, the damage microstructures consist of dislocation tangles and small cavities at all test temperatures. The concentrations of these cavities are at least three to four orders of magnitude greater than those for the corresponding single ion bombardments. And the majority of the cavities created by the multiple beam bombardments are much smaller than the ones formed by the single beam. These cavities show modest coarsening with increasing bombardment temperature. At 500 and 550°C a small fraction of them exhibit exaggerated growth. At 600°C there are many cavities but no obvious radiation-induced increase in dislocation density, and no bimodal cavity growth. The experiment made with the dual iron and helium beams shows that the absence of deuterium does not inhibit the very considerable promotion of cavities caused during the multiple beam bombardments.

The numerous cavities seen at grain boundaries, where bias-driven cavities cannot be sustained because of the very low supersaturations of point defects there, must be helium bubbles. This raises the question of whether the matrix cavities are bubbles, too. We calculated the amounts of helium required to support the cavity populations as equilibrium bubbles using the Van der Waals' expression and an assumed surface energy of $2 J/m^2$. Grain boundary bubbles were included. The required helium levels and implanted helium levels were found to agree within a factor of 2, which is within the experimental error for the cavity measurements. So the cavities in these multiple beam bombarded specimens

could all be helium stabilized. Certainly, there is enough helium to initiate all of the cavities. However, there are good reasons for believing that the larger cavities in the bimodal size groups in the 500 and 550°C specimens are bias-driven cavities, not equilibrium bubbles. First, such bimodal size spectra are good demonstrations of the critical size concept of bias-driven growth [5,6]. Here, cavity nuclei, stabilized by gases, reach a critical size or a critical gas content beyond which the net rate of input of vacancies to the cavities exceeds the net emission rate and the cavities experience a sudden increase in growth rate without need of further influx of gas. In this view, the small, persistent cavities are gas bubbles that are somewhat inflated above their thermal equilibrium sizes by radiation-produced vacancies but have not yet reached the prevailing critical size. The larger cavities are those that have passed the critical size and are growing by accepting the excess vacancies remaining when interstitial atoms are preferentially absorbed at dislocations. The fact that the subcritical cavities are large enough to be seen easily by TEM suggests a large critical size. This would result from a high recombination rate of point defects, which is consistent with the low levels of swelling. The second reason for claiming bias-driven growth of the larger cavities is that the corresponding grain boundary cavities did not exhibit a bimodal growth pattern. If the large matrix cavities were really gas bubbles formed by sporadic coalescence of small bubbles, there seems to be no good reason why such growth should not occur in the grain boundary bubbles, too. On the other hand, bias-driven growth is highly unlikely in the grain boundary bubbles, as mentioned earlier. The third and final argument for bias-driven growth is the absence of a bimodal growth mode at the higher temperature of 600°C where bubble coalescence should be more likely but where the radiation-induced dislocations

needed to sustain the bias are not available. We conclude that the larger cavities caused by the multiple beam bombardments at 500 and 500°C are bias-driven cavities.

Consider now the cavities created in the helium-free specimens bombarded at 500 and 550°C with iron ions alone. Calculations show that about 50 appm of gas is needed to make them equilibrium bubbles. These specimens undoubtedly contained some free, residual gases. Indeed, some gas was probably necessary to initiate the cavities [5,7]. But there is no evidence indicating enough gas to provide large bubbles. There were no bubbles in the thermal control specimens nor on the grain boundaries in the bombarded specimens. And none were formed in the 600°C bombardment. Therefore, the observed cavities must be radiation-induced, bias-driven cavities. Thus these experiments define a temperature range of only 500 to 550°C for bias-driven swelling in this alloy under our bombardment conditions. This is an exceptionally narrow range compared to those encountered in other materials. Although helium broadens the temperature range for nucleation of cavities (bubbles) it does not alter the temperatures for noticeable growth. The degree of swelling is small.

The damage microstructures described herein confirm and extend the observations of Ayrault [8] who examined heavy ion damage structures in a similar alloy bombarded over the same temperature range to doses of 5–25 dpa. The cavity microstructures he describes are remarkably like the present ones, even though his bombardment conditions were different. He used nickel and helium ions without hydrogen isotopes. Furthermore, his alloy contained 1% Ni and significantly more W and Ti than the present alloy, which implies that the ion damage microstructures in this alloy are not especially sensitive to these ele-

ment . The similarity of damage structure despite the absence of deuterium in Ayrault's bombardments reinforces our conclusion that the extensive cavity formation noted in this alloy is controlled primarily by helium and does not require hydrogen (deuterium). Ayrault did no bombardments without helium, so he was not able to isolate the effects of helium.

Following Ayrault's work, several studies have been published of neutron damage in modified normalized-and-tempered Fe-9Cr-1Mo steels irradiated to dose levels of 11-36 dpa with generated helium levels of about 2-30 appm. These neutron experiments [9,10] concur in showing low-to-moderate concentrations of cavities, peak cavity development at 400°C and the introduction of new precipitate phases; there are more cavities at the higher helium levels [10]. In comparison, our ion bombardments caused very high concentrations of cavities, peak swelling at 500–550°C and no obvious radiation-affected precipitate phases. These differences can be explained by the much higher damage rates and helium levels in the ion bombardments, in accordance with theoretical expectations. The damage rates in the ion bombardments are greater by three or more orders of magnitude than those in the neutron irradiations. This mandates a shift of swelling to higher temperatures in the ion bombardments. The observed shift in the peak swelling temperature of about 125°C agrees with those measured [11] and theoretically predicted [12] for other materials. The much higher cavity concentrations in the ion bombardments are caused by the higher helium levels and the comparatively short times available for bubble migration and coalescence. The lack of precipitate formation during the ion bombardments is attributed to the relatively short bombardment times and/or the high concentrations of point defect sinks and recombination centers provided by the

dislocations and cavities; these reduce long-range transport of solute elements. Additionally, partitioning of the available quantities of solutes to the high concentrations of sinks considerably reduces the degree of solute segregation at each sink which delays or inhibits precipitation [5,6].

The narrow temperature range for bias-driven cavity growth, the low levels of swelling at these doses, and the bimodal cavity sizes characteristic of a large critical cavity size [5,6,13] all indicate a high overall recombination rate for point defects. Enhanced bulk recombination in the lattice could be induced by a high vacancy migration energy [14]; it could also be raised by trapping of point defects at solute atoms [14,15]. Recombination at sinks is increased by a high sink density or by strongly imbalanced cavity and dislocation sink strengths [16]. A weak dislocation bias will also encourage recombination. Suggested causes of weak bias in ferritic materials include competing types of dislocation loops [17], impurity pinning of dislocations [18] and a smaller difference in the relaxation volumes of vacancies and interstitials [19]. Unfortunately, our experiments allow no test of these different mechanisms. For the specific case of this class of normalized-and-tempered steels, Ayrault [8] contends that swelling is low because of the small lath sizes. The lath boundaries are viewed as the primary point defect sinks. Their effectiveness in reducing the point defect levels is particularly strong in the narrower laths where their ranges of influence overlap strongly. Thus, the conditions for bias-driven growth of cavities are better in the wider laths. This explanation can account for our observations that the bias-driven cavities were most common in the larger laths and that none were seen really close to the lath boundaries. A further consideration is that the lath boundaries will drain helium from the lath interiors, diminishing the

chances of creating critical-size cavities in the laths, especially in the narrower laths. However, lath boundaries should not be regarded as the sole source of swelling resistance in this alloy. Rather, they are only a contributory factor since large-grained ferritic materials have good resistance to swelling, too [1].

Two other factors are considered to contribute to the low swelling response of this alloy. These are the high initial dislocation density created during the heat treatment and the very high concentrations of cavities generated during the multiple beam bombardments. Both of these features increase the sink densities and can affect the balance of vacancy and interstitial sink strengths. The grown-in dislocations will enhance recombination of point defects from the very beginning of the bombardments and will influence the trapping of helium and the formation of bubbles. Although the presence of helium causes more swelling than in the helium-free condition, the level of swelling will be restricted if the cavities at high concentration are the dominant point defect sinks. Assuming that the capture efficiencies of dislocations and cavities for point defects are roughly equal, a measure of the respective sink strengths is given by ρ_d, the dislocation density, and $2\pi N\bar{d}$, where N is the concentration of cavities of mean diameter, $\bar{d}$. Swelling will be a maximum when these terms are equal [16], i.e. when $\rho_d/2\pi N\bar{d} = 1$. A significant deviation from unity in this ratio will reduce the rate of swelling. Sink strength ratios are given in the last column of Table 1. It is clear from a perusal of these that the ratios for the no-gas bombardments are very high, consistent with swelling suppression by dislocations, whereas those for the multiple beam bombardments are less than unity, indicative of the dominant role of cavities. In only one case, the triple beam bombarded specimen at 500°C, does the sink strength ratio approach

unity. The level of swelling in this specimen is not high but the dose it received is relatively low and it was consequently subjected to higher gas/dpa ratios than the other multiple beam bombarded specimens. The influence of these bombardment parameters is not clear. The significance of this specimen in terms of its sink strength ratio is that it indicates that a balanced sink strength situation is achievable in this alloy, and that the specimen may be poised for continued bias-driven swelling if it can maintain its ratio at or near unity. The implication is that the good swelling resistance of this alloy may not be permanent.

The prior austenite and lath boundaries in the multiple beam bombarded specimens are covered with small helium bubbles whose mean diameter increases about 40% between 500 and 600°C but whose planar concentrations seem to be insensitive to bombardment temperature. Typically, the center-to-center spacing of these grain boundary bubbles is only about 10 nm. Assuming them to be equilibrium bubbles, it is estimated that they contain about 10% of the implanted helium contents at 500°C, rising to about 30% at 600°C. This increase agrees roughly with the corresponding increase in the width of the cavity-depleted regions adjacent to the grain boundaries. The large fractions of helium accommodated in the grain boundary bubbles are due to the small grain (lath) size. The question of whether these bubbles will pose a serious threat to intergranular cohesion in this alloy under elevated temperature creep conditions needs to be addressed.

REFERENCES

[1] Little, E.A. and Stow, D.A., *Journal of Nuclear Materials*, Vol. 87, 1979, p. 25.

[2] Klueh, R.L. and Vitek, J.M., *Journal of Nuclear Materials*, Vol. 117, 1983, p. 295.

[3] Sikka, V.K., Ward, C.T., and Thomas, K.C., p. 65–84 in *Ferritic Steels for High Temperature Applications*, Ed., S.K. Khare, Pub. American Society for Metals, 1983.

[4] Farrell, K., Lewis, M.B., and Packan, N.H., *Scripta Metallurgica*, Vol. 12, 1978, p. 1121.

[5] Mansur, L.K. and Coghlan, W.A., *Journal of Nuclear Materials*, Vol. 119, 1983, p. 1.

[6] Farrell, K., Maziasz, P.J., Lee, E.H., and Mansur, L.K., *Radiation Effects*, Vol. 78, 1983, p. 277.

[7] Farrell, K., *Radiation Effects*, Vol. 53, 1980, p. 175.

[8] Ayrault, G., *Journal of Nuclear Materials*, Vol. 114, 1983, p. 34.

[9] Gelles, D.S. and Thomas, L.E., p. 343 in *Alloy Development for Irradiation Performance Semiannual Progress Report for Period Ending March 31, 1982*, U.S. Dept. of Energy Publication ER-0045/8, Sept. 1982.

[10] Vitek, J.M. and Klueh, R.L., *Proceedings of Third Topical Meeting on Fusion Reactor Materials*, Albuquerque, New Mexico, Sept. 19–22, 1983 (in press).

[11] Packan, N.H., Farrell, K. and Stiegler, J.O., *Journal of Nuclear Materials*, Vol. 78, 1978, p. 143.

[12] Mansur, L.K., *Journal of Nuclear Materials*, Vol. 78, 1978, p. 156.

[13] Horton, L.L. and Mansur, L.K., pp. , this proceedings.

[14] Mansur, L.K., *Journal of Nuclear Materials*, Vol. 83, 1979, p. 109.

[15] Hayns, M.R. and Williams, T.M., *Journal of Nuclear Materials*, Vol. 74, 1978, p. 151.

[16] Mansur, L.K., *Nuclear Technology*, Vol. 40, 1978, p. 5.

[17] Bullough, R., Wood, M.H., and Little, E.A., p. 593, in *Effects of Radiation of Materials: Tenth Conference*, ASTM STP 725, Eds. D. Kramer, H.R. Brager, and J.S. Perrin, American Society for Testing and Materials, 1981.

[18] Little, E.A., *Journal of Nuclear Materials*, Vol. 87, 1979, p. 11.

[19] Sniegowski, J.J. and Wolfer, W.G., *Proceedings of Conference on Ferritic Alloys for Use in Nuclear Energy Technologies*, Snowbird, Utah, June 19–23, 1983 (in press).

TABLE 1 — Specific bombardment conditions and measured microstructural data.

Temp., °C	dpa	Helium, appm	Deuterium, appm	Cavities					Dislocation density, ρ_d, m/m^3	$\rho_d/2\pi N\bar{d}$
				Within grains			On grain boundaries			
				Concentration N/m^3	Diameter $\bar{d}$, nm	Swelling, %	Concentration N/m^2	Diameter $\bar{d}$, nm		
404–408	110	-0-	-0-	-0-	...	-0-	-0-	...	Dense tangles	...
403–410	106	1040	4640	$\sim 2\times10^{23}$	~2.0	0.08	ND	...	Dense tangles	...
450–460	95	-0-	-0-	-0-	...	-0-	...	...	Dense tangles	
452–456	94	920	4100	$\sim 1.6\times10^{23}$	2.3	0.10	D	...	Dense tangles	...
491–494	93	-0-	-0-	$<3\times10^{19}$	~25.	<0.02	-0-	...	5×10^{14}	106
				5.3×10^{22} / 7×10^{21}	2.1 / 7.6	0.03 / 0.17	...	...	...	...
502–503	54	890	3950				8×10^{15}	1.9	9×10^{14}	0.9
				2.9×10^{23} / 3.8×10^{21}	2.6 / 8.9	0.27 / 0.14	...	...	...	...
498–500	121	990	-0-				1.3×10^{16}	1.9	7×10^{14}	0.14
545–547	116	-0-	-0-	$<4\times10^{18}$	~60.	<0.05	-0-	...	4×10^{14}	267
				5.1×10^{22} / 1.4×10^{21}	3.7 / 9.3	0.13 / 0.06				
550–552	104	870	3880				9.3×10^{15}	2.6	9×10^{14}	0.6
597–603	106	-0-	-0-	-0-	...	-0-	-0-	...	$2–3\times10^{14}$	...
590–595	95	940	4180	4×10^{22}	4.0	0.13	1×10^{16}	2.7	$2–3\times10^{14}$	0.25

ND = No cavities discerned.

D = Just discernible but not countable.

FIGURE CAPTIONS

Fig. 1. Dislocations and lath boundaries in normalized-and-tempered Fe-9Cr-1Mo-Nb-V steel.

Fig. 2. Cavity distributions after bombardment to a) 93 dpa at 500°C with Fe ions; b) 121 dpa at 500°C with Fe + He ions. c) Uniform size cavities after 95 dpa at 600°C with Fe + He + D ions.

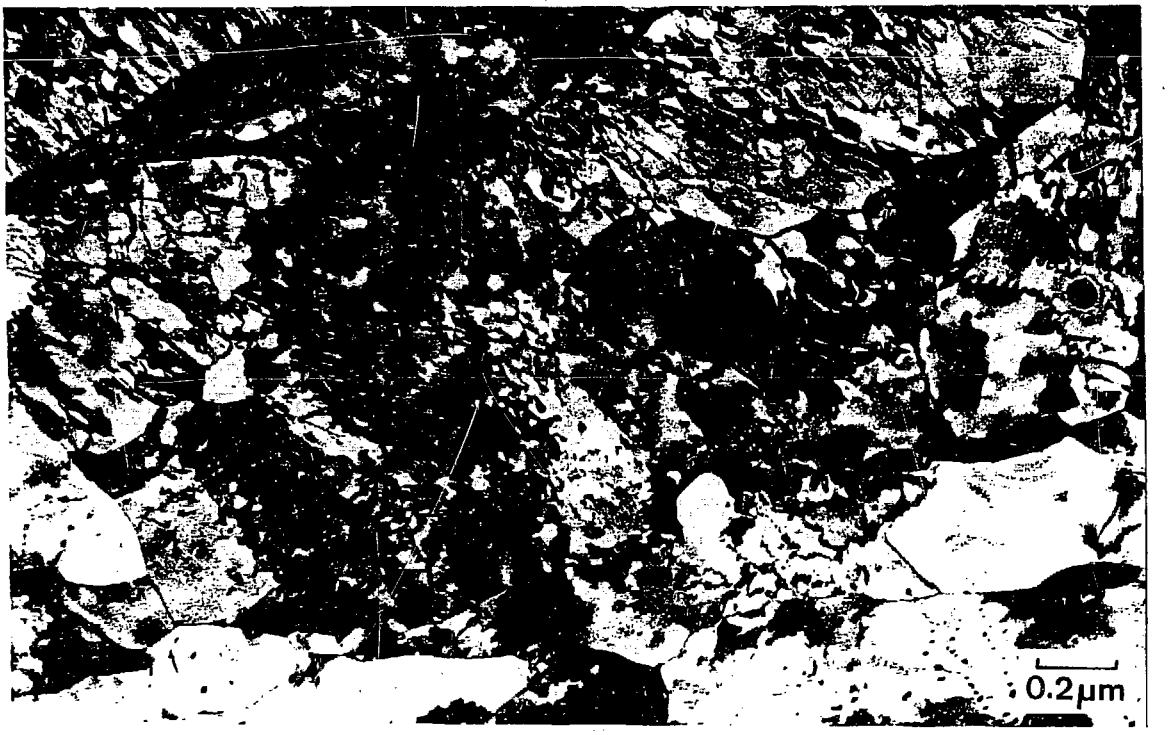

Fig. 1. Dislocations and lath boundaries in normalized-and-tempered Fe-9Cr-1Mo-Nb-V steel.

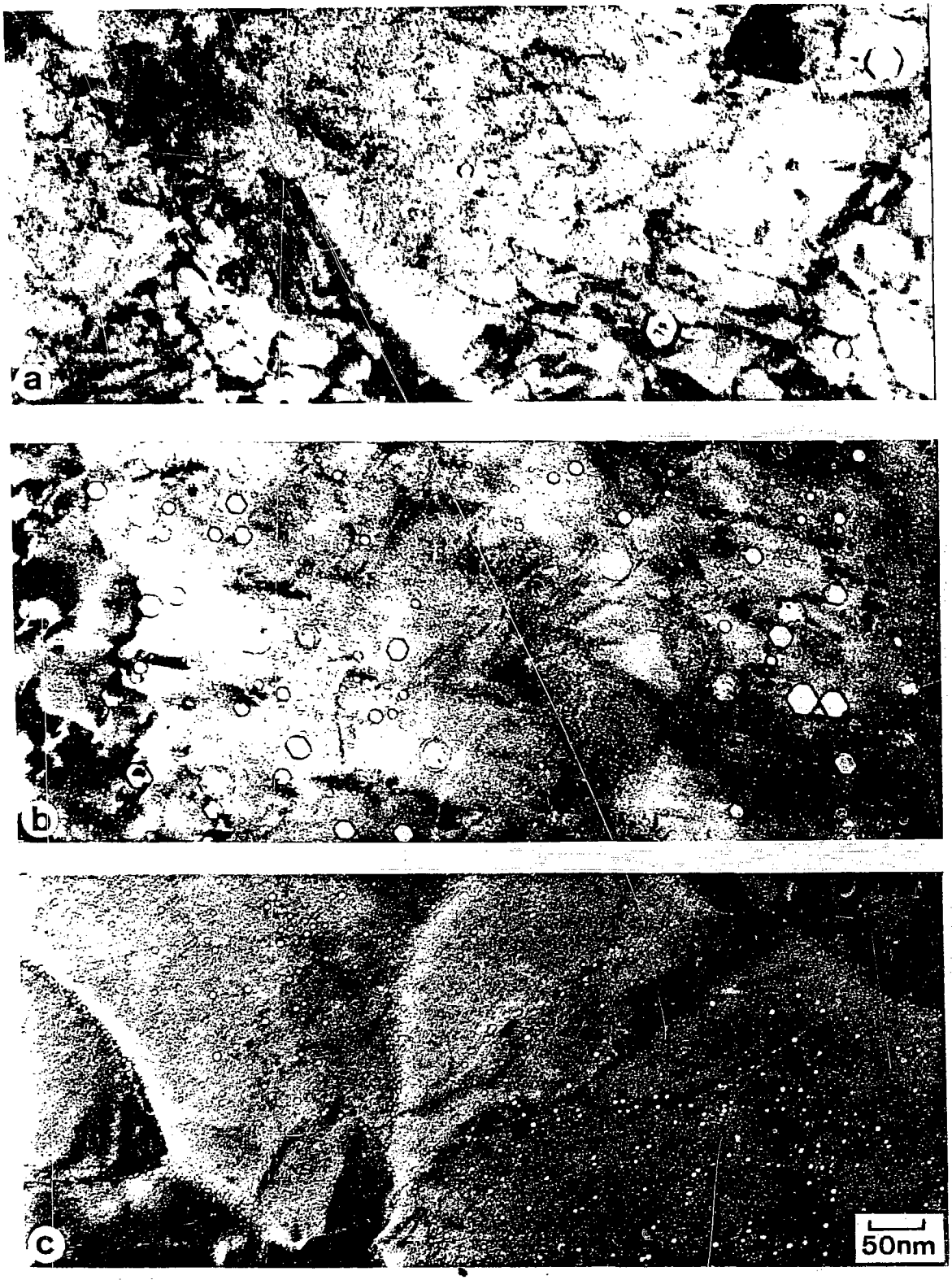

Fig. 2. Cavity distributions after bombardment to a) 93 dpa at 500°C with Fe ions; b) 121 dpa at 500°C with Fe + He ions. c) Uniform size cavities after 95 dpa at 600°C with Fe + He + D ions.